Annales
Geophysicae

Multi-year observations of gravity wave momentum fluxes at low and middle latitudes inferred by all-sky meteor radar

V. F. Andrioli[1], P. P. Batista[1], B. R. Clemesha[1], N. J. Schuch[2], and R. A. Buriti[3]

[1]Instituto Nacional de Pesquisas Espaciais – INPE, São José dos Campos, SP, Brazil
[2]Centro Regional Sul de Pesquisas Espaciais, Santa Maria, RS, Brazil
[3]Universidade Federal de Campina Grande, Campina Grande, PB, Brazil

Correspondence to: V. F. Andrioli (vania@laser.inpe.br)

Abstract. We have applied a modified composite day analysis to the Hocking (2005) technique to study gravity wave (GW) momentum fluxes in the mesosphere and lower thermosphere (MLT). Wind measurements from almost continuous meteor radar observations during June 2004–December 2008 over São João do Cariri (Cariri; 7° S, 36° W), April 1999–November 2008 over Cachoeira Paulista (CP; 23° S, 45° W), and February 2005–December 2009 over Santa Maria (SM; 30° S, 54° W) were used to estimate the GW momentum fluxes and variances in the MLT region. Our analysis can provide monthly mean altitude profiles of vertical fluxes of horizontal momentum for short-period (less than 2–3 h) GWs. The averages for each month throughout the entire data series have shown different behavior for the momentum fluxes depending on latitude and component. The meridional component has almost the same behavior at the three sites, being positive (northward), for most part of the year. On the other hand, the zonal component shows different behavior at each location: it is positive for almost half the year at Cariri and SM but predominantly negative over CP. Annual variation in the GW momentum fluxes is present at all sites in the zonal component and also in SM at 89 km in the meridional component. The seasonal analysis has also shown a 4-month oscillation at 92.5 km over SM in the zonal component and over CP at the same altitudes but for the meridional component.

Keywords. Meteorology and atmospheric dynamics (middle atmosphere dynamics)

1 Introduction

It is widely accepted that atmospheric gravity waves (GWs) are responsible for the energy and momentum transport from the lower to the upper atmosphere. Additionally, the deposition of this energy and momentum by wave breaking plays a crucial role in the dynamics and energy balance of the mesosphere and lower thermosphere (MLT) region. In this context the Hocking (2005) technique has helped in making plenty of data sites around the world available, leading to a better understanding of the morphology of global gravity wave-induced momentum fluxes. This is because the technique makes it possible to infer the components of momentum flux and wind variance from all-sky meteor radar data and, according to Hocking (2005) at the time of writing, there were almost 30 such radars distributed worldwide.

In recent years the results of a number of studies have been published using the Hocking technique, e.g., Antonita et al. (2008), Fritts et al. (2010, 2012a, b.), Placke et al. (2011a, b), Andrioli et al. (2013a, b) and de Wit et al. (2014a, b). Andrioli et al. (2013a) described a method for using the technique in composite days with the purpose of maximizing the number of available meteor echoes and thus allowing the investigation of momentum fluxes using simple meteor radars with improved accuracy and with no contamination by tides and planetary waves. Although this method does not allow momentum fluxes with high time resolution to be inferred, we can at least investigate the monthly mean and the seasonal variation in the fluxes without tide and planetary wave contamination. We have used data from three VHF all-sky interferometric meteor radars ranging from low to middle latitudes over the Brazilian sector of the Southern Hemisphere. In an earlier paper, Clemesha et al. (2009) analyzed
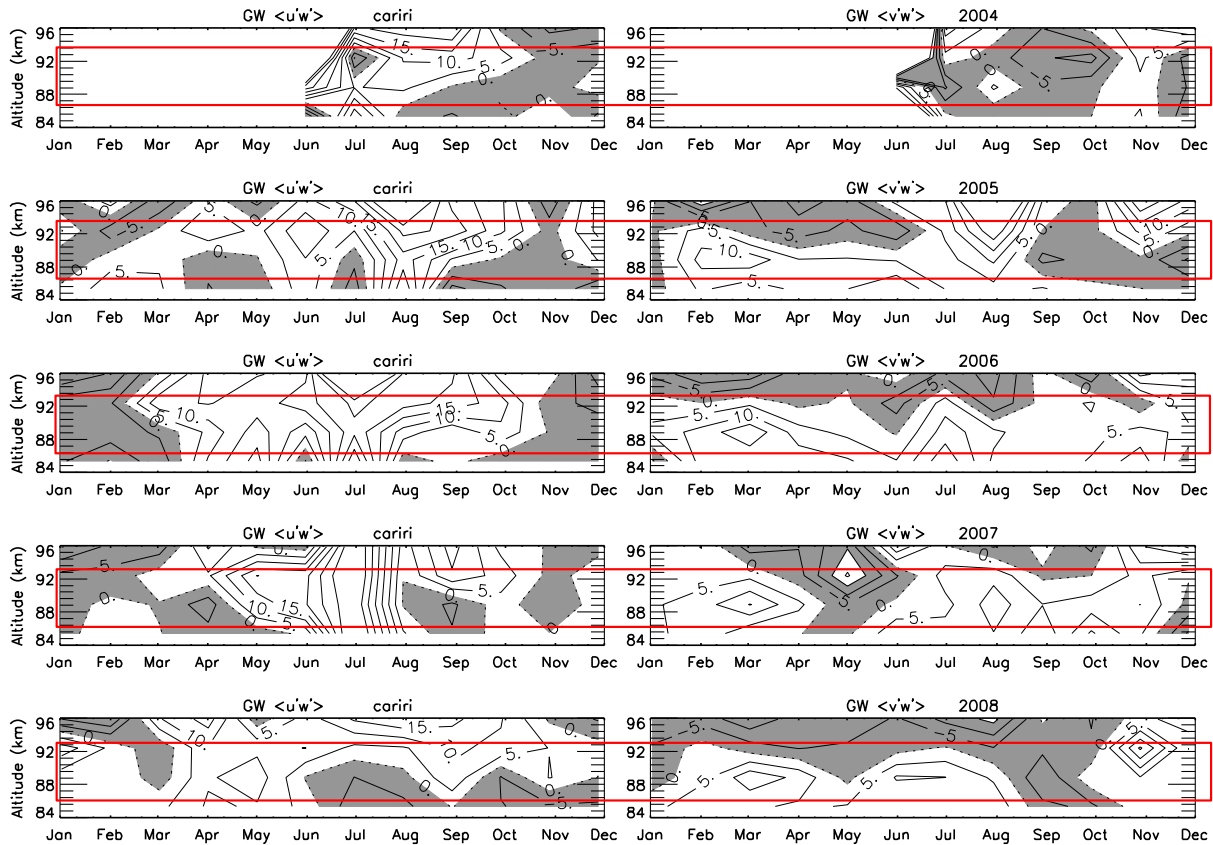
Figure 1. Monthly mean vertical profiles of GW momentum fluxes from 2004 (top) to 2008 (bottom): zonal (left) and meridional (right) components. Each contour corresponds to $5\,\mathrm{m^2\,s^{-2}}$; the white areas represent positive values and grey the negative. Dashed lines show where the values are zero. These panels represent the results for Cariri from 2004 to 2008.

wind variances in this region but with only 1 year of data. In this paper we extend the analysis over all available data as well as studying not only wind variances but also momentum fluxes.

2 Methods

According to Andrioli et al. (2013a) it is possible to infer the GW momentum fluxes and variances with a good accuracy using simple all-sky meteor radar data. We do this by using a modified composite day (MCD) method applied to the Hocking (2005) analysis. We have applied MCD analysis to the meteor radar data from three sites located at São João do Cariri (Cariri; 7° S, 36° W), Cachoeira Paulista (CP; 23° S, 45° W) and Santa Maria (SM; 30° S, 54° W). The data were analyzed using height intervals of 4 km with a 3 km displacement between adjacent intervals (centered on 82, 85.5, 89, 92.5 and 96 km), a 3 h time interval with a 2 h displacement (centered at 01:00, 03:00, 05:00, 07:00, 09:00, 11:00, 13:00, 15:00, 17:00, 19:00, 21:00 and 23:00 UT), and zenith angles between 15 and 50°. The latter constraint avoids large spurious contributions to apparent GW variances due to large vertical velocities at small zenith angles and range errors due to

zenith angle uncertainties at low elevation angles. This analysis allows us to study GWs with periods less than ∼ 3 h, vertical wavelengths less than ∼ 5–10 km, and horizontal wavelength less than ∼ 180 km. Additional details of the method can be found in Andrioli et al. (2013a).

Our analysis employs all available data for each of the meteor radars: Cariri from 2004 to 2008, CP from 1999 to 2008 and SM from 2005 to 2009. The figures showing these data series with data gaps are shown in Andrioli et al. (2013b) (Figs. 1, 2, and 3 for Cariri, CP, and SM, respectively). We can see from those figures that there are approximately 4, 9, and 5 years of data for Cariri, CP, and SM, respectively. Besides seasonal analysis, we also averaged all these data in order to get a pattern of behavior for the momentum fluxes over each location. The results presented in the following represent vertical profiles of monthly means both for variances and for moment flux.

3 Results

Figure 1 shows the components of the monthly mean vertical profiles of the GW momentum fluxes over Cariri. The panels shown on the left side of this figure correspond to
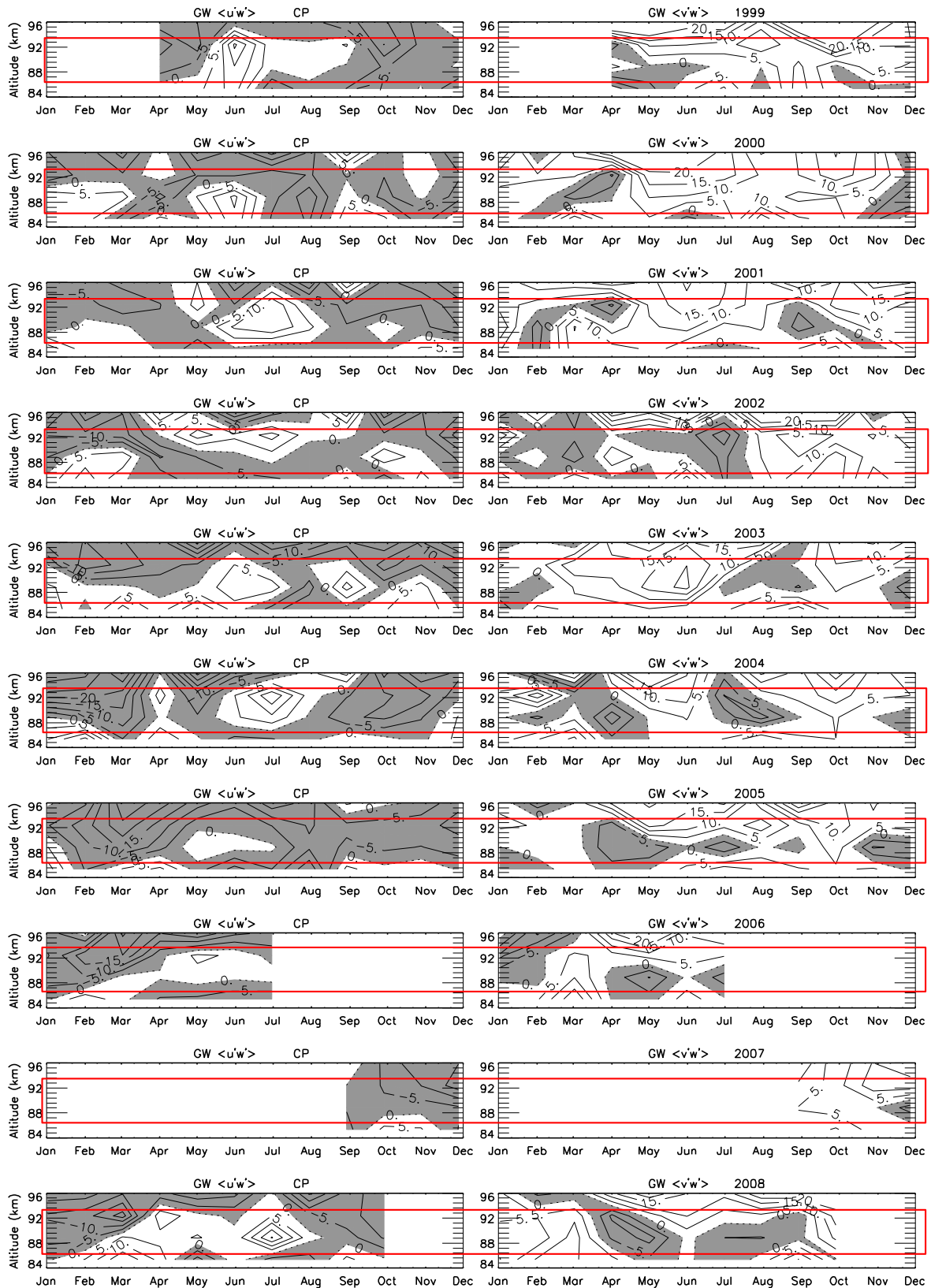
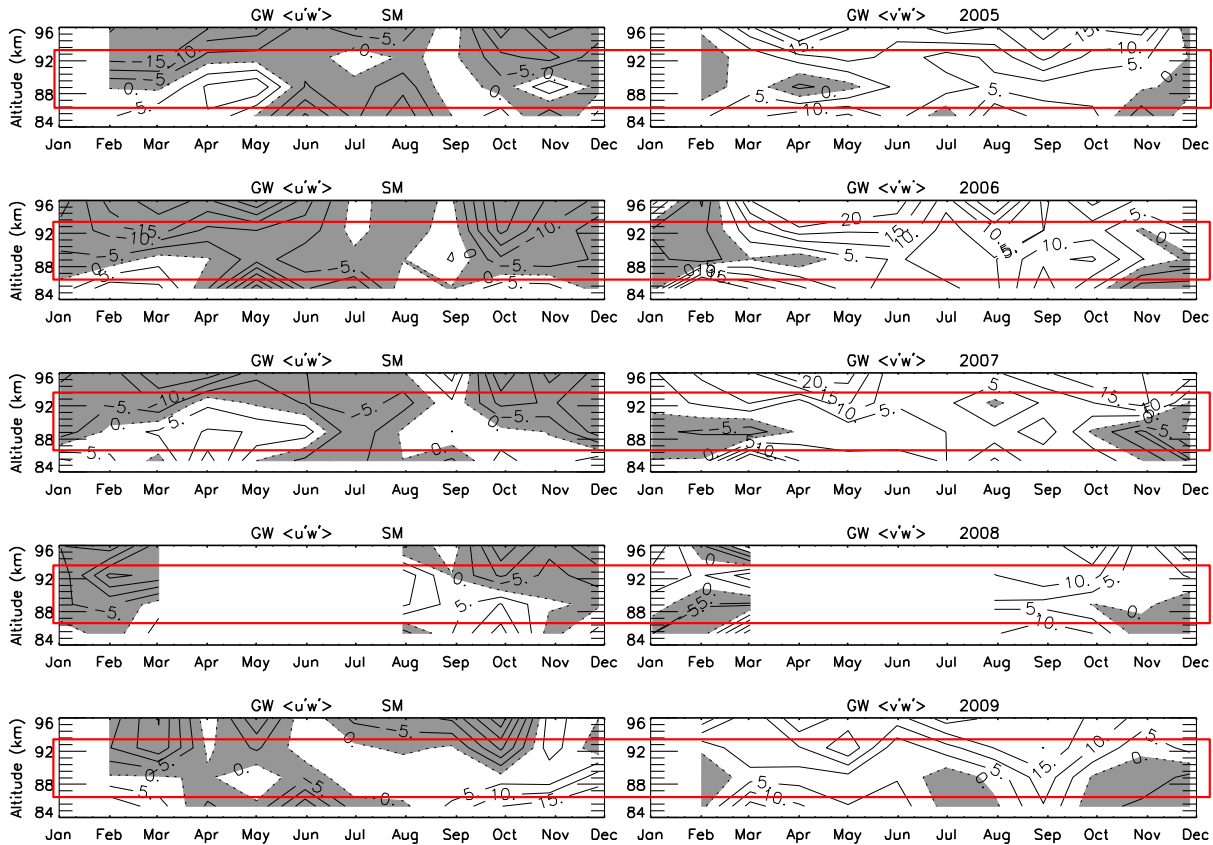**Figure 2.** The same as Fig. 1 but for Cachoeira Paulista from 1999 to 2008.

Figure 3. The same as Fig. 1 but for Santa Maria from February 2005 to 2009.

the zonal component ($<u'w'>$), and those on the right to the meridional ($<v'w'>$). According to the tests presented by Andrioli et al. (2013a), we can expect better reliability in the results from 87 to 94.4 km altitude layers, centered on 89 and 92.5 km, where the meteor counts are larger. We have highlighted this region with a red rectangle in all figures. For the momentum fluxes, $<u'w'>$ and $<v'w'>$, positive (white) values characterize vertical transport of eastward- and northward-directed momentum and negative values (grey) characterize westward- and southward-directed momentum. Observing mainly this region we can see some similarities and some differences in the GW momentum fluxes from one year to another. In the meridional component, we can see that the momentum fluxes diminish with increasing altitudes for almost all years, with the exception of 2005, around August, and 2004 and 2008, around November. A common positive flux (eastward) behavior can be observed in the zonal component around wintertime at higher altitudes in most years. In the zonal component we can also observe strong gradients during June 2004, July 2004, August 2005, July 2007 and August 2007. In view of the magnitude of these gradients, the data for these periods were double-checked and we found that the radar system did not work well on some days in these months. In view of this fact

we decided to treat the data points for June 2004, July 2005, August 2005, July 2007 and August 2007 as outliers, excluding them from our analysis.

The monthly mean vertical profiles of the GW momentum fluxes over Cachoeira Paulista are shown in Fig. 2. Concentrating on the altitude intervals with high accuracy, from 87 to 94.4 km, we can observe that the values for the zonal components of the momentum fluxes range from -25 to $20 \, \mathrm{m^2 \, s^{-2}}$, whereas they range from -10 to $20 \, \mathrm{m^2 \, s^{-2}}$ for the meridional component. We can observe that, from 2000 to 2003, the zonal momentum flux changes direction at around 90 km from January to April, being eastward (positive) below this altitude. The eastward direction can also be observed around the Southern Hemisphere wintertime for most years, around 91 km. The meridional component shows more year-to-year variability than the zonal, though being positive for most of the year. Moreover, with the exception of 2002, all years show an increase in the meridional momentum fluxes with altitude above 88 km around winter.

In Fig. 3 we show the momentum fluxes over Santa Maria from February 2005 to December 2009. From this figure we can clearly see a vertical gradient in the zonal component from January to April and from September to December, in most years, with changes in direction from positive
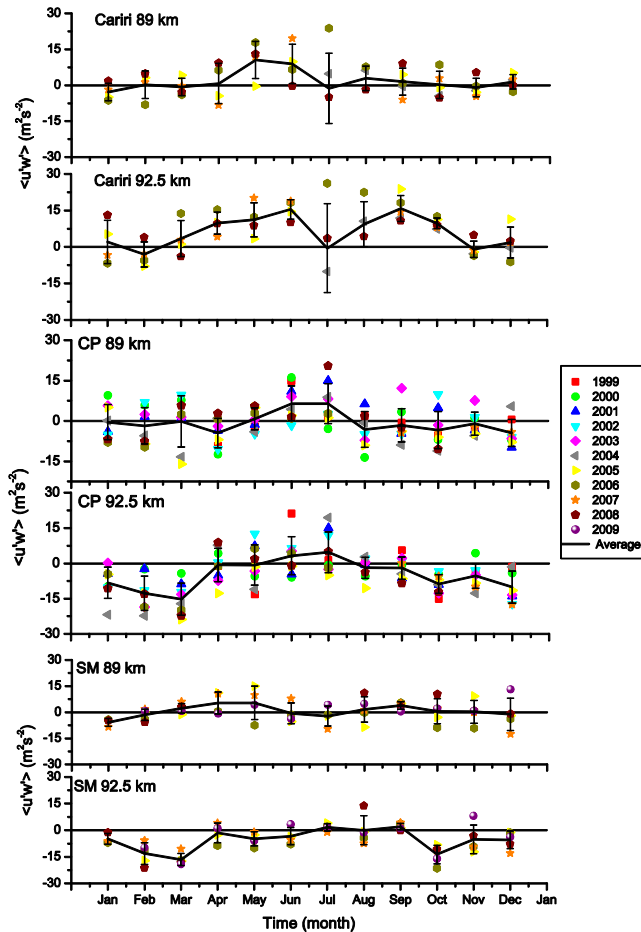
Figure 4. Monthly mean zonal momentum fluxes for the two height layers where the meteor counting rates are largest, at each site. The top panels show the results for São João do Cariri (Cariri, low latitude), the center panels are for Cachoeira Paulista (CP, middle–low latitude), and the bottom are for Santa Maria (SM, middle latitude). Error bars denote the standard deviation.

Figure 5. The same as Fig. 4 but for monthly mean meridional momentum fluxes.

to negative with increasing altitude. On the other hand, the vertical flux of meridional momentum is northward during most of the year and shows a positive gradient with altitude around winter for almost all periods of observation. In addition the absolute values are similar to those observed in CP and Cariri.

In order to distinguish possible intra-annual patterns, monthly mean momentum fluxes for all years are displayed together, in Figs. 4 and 5, for zonal and meridional components, respectively, at the two layers where the meteor rates are largest. From these figures we can see large standard deviations, at CP and Cariri mainly in the zonal component, showing that values are more spread from one year to another at these sites. Despite this, it is possible to notice a seasonal cycle at Cariri and CP with a tendency for a more eastward-directed vertical flux of zonal momentum around wintertime, and a more westward-directed flux around summertime at
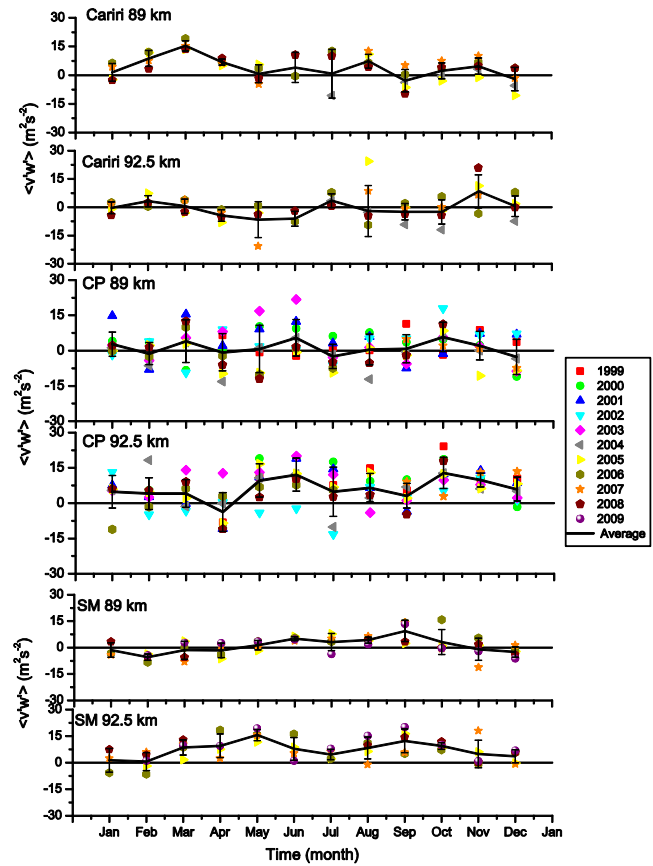
both 89 and 92.5 km. In the same component but for SM, we can observe a tendency for positive values around March and September at 89 km. In contrast, a tendency for negative values can be observed at 92.5 km, around March and October. On the other hand, in Fig. 5, the $<v'w'>$ component shows a semiannual oscillation at SM at 92.5 km, with positive maxima around the equinoxes, and an annual oscillation at 89 km with the tendency for more positive values from June to October. In addition, a tendency for more oscillatory behavior can be observed over Cariri and CP. This seasonal behavior will be discussed in more detail in Sect. 3.1.

With the aim of verifying any possible relationship between momentum fluxes measured at different stations, we have made a zero-lag 2-D cross-correlation analysis of the simultaneous observations at the three sites for all altitude levels: 85.5, 89, 92.5 and 96 km. The correlation between CP and SM was found to be 0.58 (zonal) and 0.49 (meridional), statistically significant with $p < 0.001$, for 112 data pairs. On the other hand, correlation coefficients between Cariri and SM or between Cariri and CP were statistically significant for neither zonal nor meridional components. These correlations suggest that fluxes measured at low latitudes are almost independent of those measured at middle latitudes.
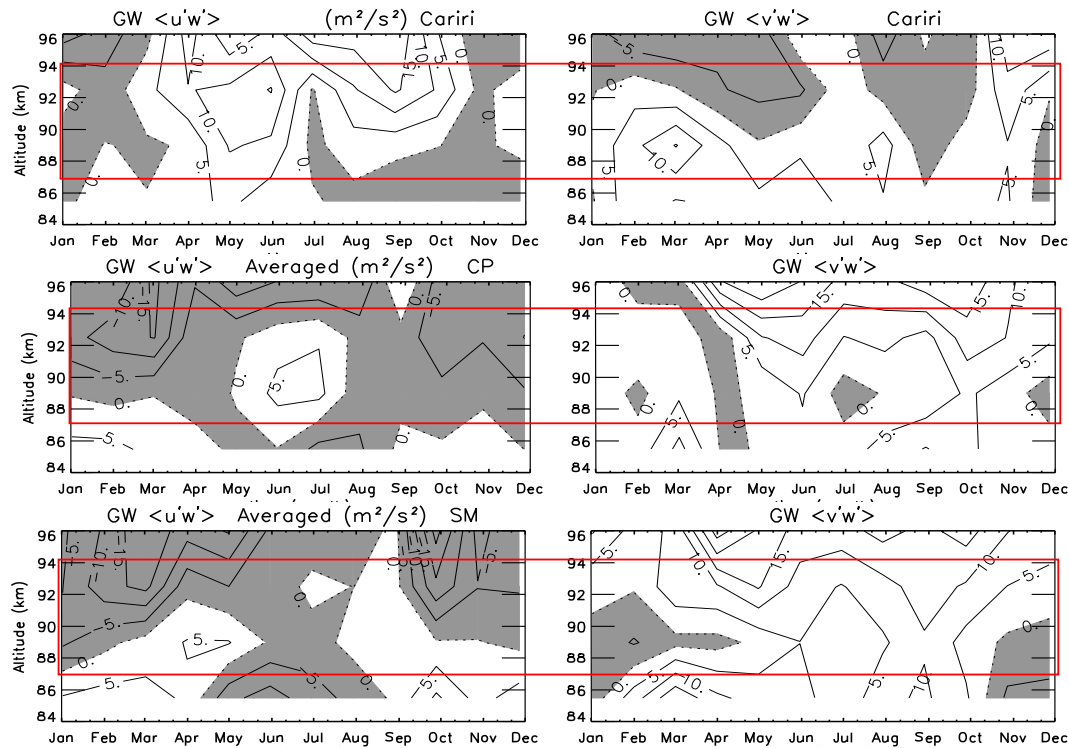
Figure 6. Averaged momentum fluxes throughout the entire available data series. Mean behavior of the vertical flux of horizontal momentum: zonal (left) and meridional (right) components. Each contour corresponds to $5\,\mathrm{m^2\,s^{-2}}$. The white areas represent positive values and grey the negative. The top panels are the results for São João do Cariri (Cariri, low latitude), the center panels are for Cachoeira Paulista (CP, mid-low latitude), and the bottom are for Santa Maria (SM, middle latitude).

In order to see any possible pattern of behavior of the momentum fluxes, winds and variances common to all years, we averaged these parameters over the entire available data set for each measurement site, and the results are shown in Figs. 6, 7 and 8, respectively. For the momentum fluxes, Fig. 6, we focus the analysis on the altitudes from 87 to 94.4 km, highlighted with a red rectangle. We can see from the right panel of this figure that the vertical transport of the meridional momentum is primarily northward throughout the year at higher latitudes, CP and SM. The flux is southward in fewer months: April (for all altitudes) and February, July and December (at 89 km) for CP, and from January to March and in November and December (below 92 km) at SM. In contrast, Cariri shows no predominantly north or south direction; instead of this it presents a tendency for more southward momentum fluxes in some regions above ~ 92 km from January to March, above 90 km around May, and for almost all altitudes from August to October. Concerning latitudinal comparison we clearly see that the meridional momentum flux has a different altitude behavior. At Cariri it is in general decreasing in altitude, but the opposite is seen for CP and SM.

Analyzing the zonal component of momentum flux, shown in the left panel of Fig. 6, we also can see similarities between patterns observed at CP and SM. For both these sites zonal

momentum diminishes with increasing altitude around summer, from November to March. On the other hand, at Cariri the vertical flux of the zonal momentum is westward from January to March, in July and from September to December at lower altitudes, and in November. At CP the vertical flux of zonal momentum is positive (eastward) only from May to July, around 90 km.

In Fig. 8, the average GW variances through the entire available data series are shown. Panels on the left and right side correspond to the zonal and meridional components, respectively. Each contour corresponds to $25\,\mathrm{m^2\,s^{-2}}$. The top panels are the results for Cariri, the center panels are for CP, and the bottom are for SM. We can observe that the meridional component is larger than the zonal. The values of the zonal component increase with increasing altitude for almost all sites throughout almost the entire year, except from May to July around 85 km altitude at CP and SM. However, we can observe maximum values from 85 to 94 km at all sites for the meridional component. Moreover, there is a clear semiannual periodicity with maximum values around the equinoxes at CP less intense at SM (see also Figure 10 and the discussion based on this figure in Sect. 3.1).
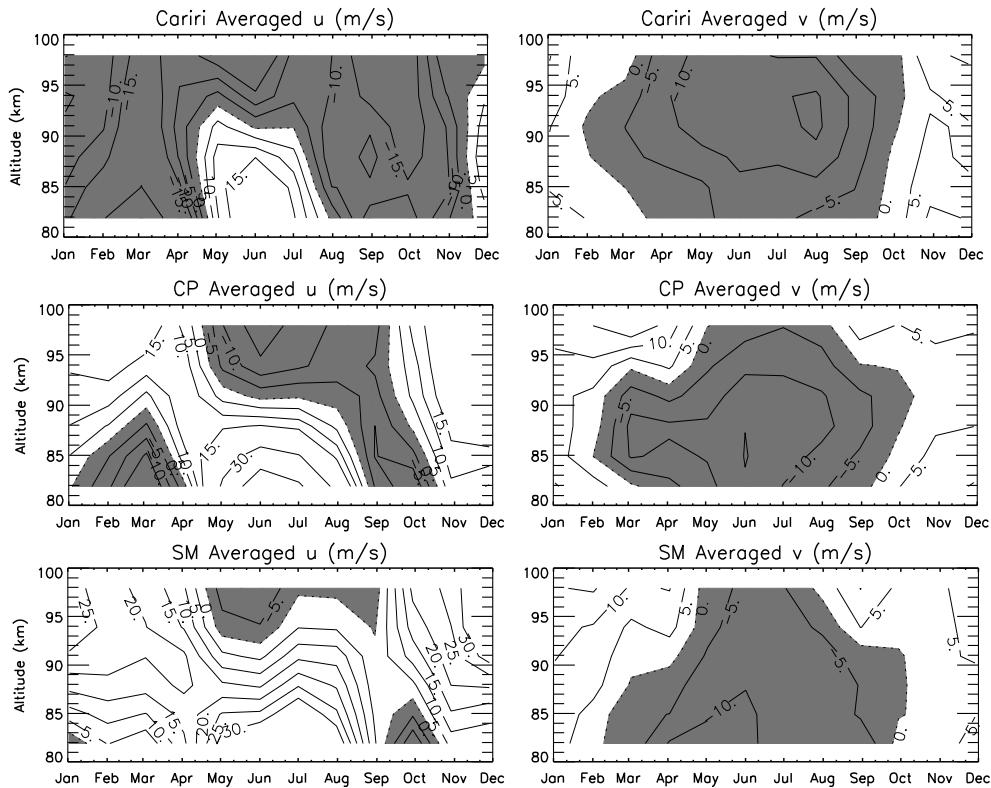
Figure 7. Averaged wind throughout the entire available data series for each site: zonal (left) and meridional (right) components. Grey means negative values and white positive. Positive values for the zonal (meridional) component correspond to eastward (northward) direction.

Seasonal analysis of GW activity

In order to investigate the seasonal behavior of the variances and momentum fluxes, we have applied a Lomb–Scargle (Scargle, 1982) periodogram analysis to the monthly mean vertical profiles of the variances, Figs. 9 and 10, and the momentum fluxes, Figs. 11 and 12, in their zonal and meridional components, respectively

Figures. 9 and 10 show the spectral analysis for GW variances in their zonal (Fig. 9) and meridional (Fig. 10) components over the three stations. The top of each figure shows the spectral analysis for Cariri, the middle panels correspond to CP and the ones on the bottom are from SM. In each of these groups the solid black line shows the analysis made using the height-averaged profile. The solid yellow line indicates 82 km, the cyan dotted line 85.5 km, the blue dashed line 89 km, the red dash-dot line 92.5 km, and the orange dash-dot line 96 km. The zonal component of the variance shows a 6-month periodicity with 90 % significance for CP at almost all altitudes; however, it does not reach the confidence level for the height-averaged profile. This is applied equally to Cariri and SM for some of the altitudes. We can see from the power spectra that the peak of the 6-month oscillation decreases its amplitude as the altitude increases at all sites. This semiannual oscillation is also seen in the meridional compo-

nent, Fig. 10, at all altitudes for SM and CP but only below 85.5 km at Cariri. Annual oscillation is seen at CP and SM for both variance components at almost all altitudes. The meridional component does not show statistically significant periodicity in the height-averaged profile over Cariri.

Figures 11 and 12 show the spectral analysis of the zonal and meridional components, respectively, of the momentum fluxes over the three stations. In this case, the analysis has been done only for the altitudes where we have more reliability – that is, 89 km (blue dashed line) and 92.5 km (red dash-dot line). The analysis over the height-averaged series of $<u'w'>$, Fig. 11, shows an annual variation reaching the 90 % confidence level over Cariri and CP; however, in SM only 4- and 12-month oscillations can be seen at 92.5 km. Also, we can see that the amplitude of the annual oscillation increases with height for both Cariri and CP.

The meridional component, Fig. 12, shows an annual oscillation over SM at 89 km altitude. It also shows a 4-month oscillation over CP, reaching the 90 % significance level at 92.5 km. The emergence of a terannual oscillation is surprising because there has been no earlier report of this oscillation in the GW momentum flux seasonal analysis. Nonetheless, there are some studies reporting this oscillation in other parameters related to dynamics in the MLT region, such as the mean wind and tides (Iimura et al., 2010), kinetic energy dis-
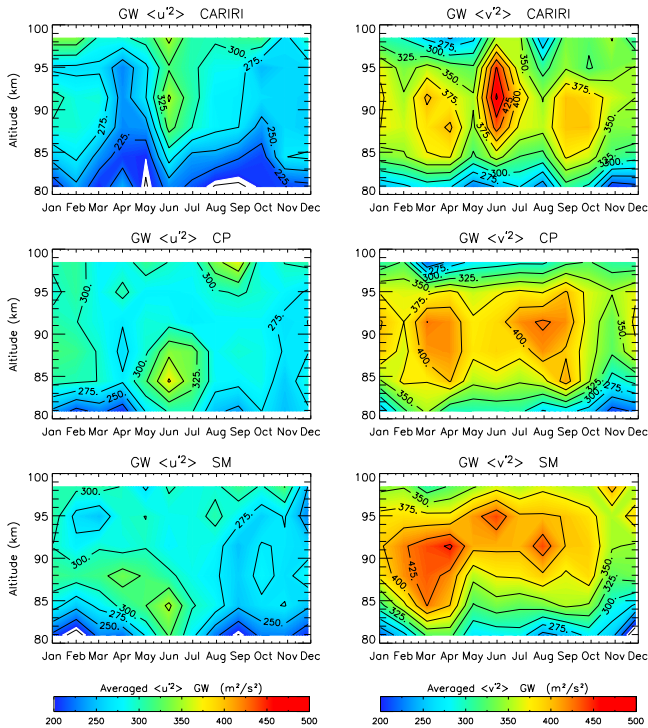
Figure 8. Averaged GW variances throughout the entire available data series: zonal (left) and meridional (right) components. Each contour corresponds to $25\,\mathrm{m^2\,s^{-2}}$. The top panels are the results for São João do Cariri (Cariri, low latitude), the center panels are the results for Cachoeira Paulista (CP, mid–low latitude), and the bottom panels are the results for Santa Maria (SM, middle latitude).

Figure 9. Lomb–Scargle spectral analysis of zonal component of GW variance over São João do Cariri (top), Cachoeira Paulista (middle), and Santa Maria (bottom). The horizontal straight green lines show the 90 % confidence levels. For all stations the solid black line represents the height-averaged profile, the solid yellow line 82 km, the cyan dotted line 85.5 km, the blue dashed line 89 km, red dash-dot line 92.5 km, and the orange dash-dot line 96 km.

sipation rates (Hall et al., 2003) and nighttime airglow emissions (Fukuyama, 1977).

Harmonic analysis (not shown in this paper) indicates that annual oscillation of the $<u'w'>$ component has a maximum around June at all the three sites. The 4-month oscillation seen in the $<v'w'>$ component has a maxima in February, June and October at CP. Comparing the results from variances with those from momentum fluxes, we can see the same seasonal behavior, showing annual oscillation, only at 89 km for SM with respect to the meridional variance and momentum flux. On the other hand, it should be remembered that the GWs that most contribute to the momentum fluxes are the high-frequency GW, whereas for variances (energy transport) the low-frequency GWs are most important (see Fritts and Alexander, 2003, for more details).

4 Discussion

According to Lindzen (1981), GWs encounter a critical level when the background wind approaches the phase speed of the wave. Owing to the small horizontal phase speeds of GWs, which is of the order of the background mean flow, GWs are very sensitive to background wind filtering in the middle atmosphere (Placke et al. 2011a). In general a GW can
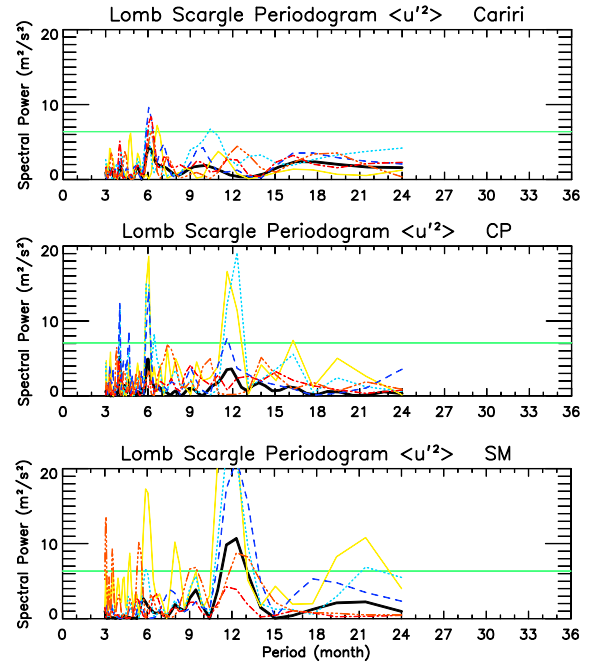
propagate only against the wind; otherwise it would have encountered a critical level in the mesosphere. If eastward wind is prevailing, only westward-propagating GWs with negative zonal momentum fluxes can move vertically, and vice versa. From the right panels of Fig. 6 we can observe that northward-directed vertical momentum flux occurs mainly where southward meridional wind (right panels of Fig. 7) is prevailing around winter. This shows the coupling between background winds and momentum fluxes.

Coupling between zonal momentum fluxes and background wind can be analyzed by comparing the results shown in the left panels of Fig. 6 with those shown in Fig. 7. We can clearly see at SM, from May to August, that the zonal wind and GW $<u'w'>$ are in opposite directions, allowing vertical propagation for GW. It should be pointed out that the wind reversal observed over SM, from April to September around 95 km, could also be due to other wave interactions or even to GW breaking, but with frequencies different to those observed in our analysis. Inspecting CP and SM from January to April, and November to December below 88.5 km, $<u'w'>$ is positive and diminishes with increasing altitude, and as a consequence of a moment transfer to the mean flow, an eastward acceleration can be observed in the zonal wind. On the other hand, the meridional wind (right-hand side of Fig. 7) is negative from May to August at the three sites,
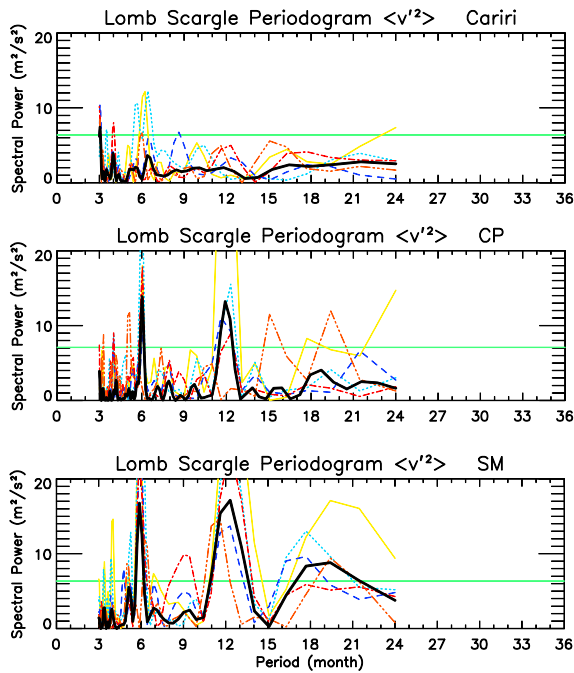
Figure 10. The same as Fig. 9 but for the meridional variance component.

Figure 11. Lomb–Scargle spectral analysis of zonal component of GW momentum fluxes over São João do Cariri (top), Cachoeira Paulista (middle), and Santa Maria (bottom). The horizontal green straight lines show the 90 % confidence levels. In all stations the solid black line represents the height-average profile, the blue dashed line corresponds to 89 km altitude and the red dash-dot line corresponds to 92.5 km altitude.

and the $<v'w'>$ (right-hand side of Fig. 6) is generally positive in this period below 90 km, indicating that the conditions for GW vertical propagation are allowable around winter. In other words, GW propagating in a north–south direction can reach higher altitudes during the wintertime for all three sites.

According to Sato et al. (2009, 2011) in their gravity-wave-resolving general circulation model, an annual variation in the zonal momentum fluxes can be observed at 0.1 hPa (a height of about 64 km) for the same latitudes as Cariri, CP and SM. Moreover, the flux is positive for the summertime and the wind is negative, leading to a condition favorable for upward gravity wave propagation at latitudes around 30° S. Comparing this to the left-hand side of Fig. 6, we can see positive values of zonal flux around summer at lower altitudes for both CP and SM, agreeing with their results. Moreover, both sites show an annual behavior agreeing with the models results for the mesosphere.

Fukuyama (1977), in his statistical study on night airglow emissions around the mesopause region, found fluctuations of 12-, 6- and 4-month periods. A study of seasonal GW activity over the three Brazilian meteor radar sites was also made by Clemesha et al. (2009). In their work they analyzed the fluctuating wind velocities related to GW and observed a semiannual oscillation (SAO) in the meridional wind component over CP and SM, agreeing with our results for the variances (Fig. 10). Antonita et al. (2008), also using Hocking's analysis, found a SAO for the GW momentum fluxes with maxima at the equinoxes, over Trivandrum (8.5° N, 76.9° E). In the present study, no statically significant SAO in momen-
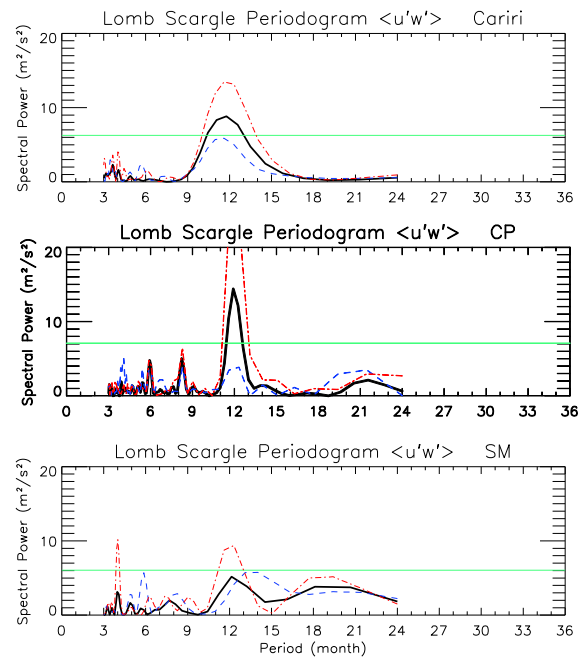
tum fluxes has been observed. Mitchell and Beldon (2009) observed a SAO with maxima at the solstices at Rothera (68° S, 68° W) and Beldon and Mitchell (2009) observed the same behavior for Esrange (68° N) for the fluctuating radial velocities. Senft and Gardner (1991) observed annual and SAO in GW activity at Urbana (40° N, 88° W) using Na lidar data to infer atmospheric density perturbations and their spectra. These results are similar to those found by us for middle latitudes, corresponding to SM and CP, the latter mainly in the meridional component of the variances. Placke et al. (2011b) in their analysis of GW activity over Andenes (69.3° N, 16° E) and Juliusruh (54.6° N, 13.4° E) report SAO with maxima around the solstice. As stated earlier, annual and semiannual oscillations in GW activity are anticipated and have been documented in earlier work (e.g., Antonita et al.,2008; Clemesha et al., 2009; Mitchell and Beldon, 2009; Beldon and Mitchell, 2009; Senft and Gardner, 1991; Placke et al., 2011b; De Wit et al., 2014b; and references therein); however, this appears to be the first report of a 4-month oscillation in GW momentum fluxes.

Although what appear to be real terannual oscillations have been reported by some other authors in several dynamical parameters in the MLT region (Fukuyama, 1977; Hall et al., 2003; Iimura et al., 2010), no plausible mechanism for driving atmospheric dynamics with a 4-month period has
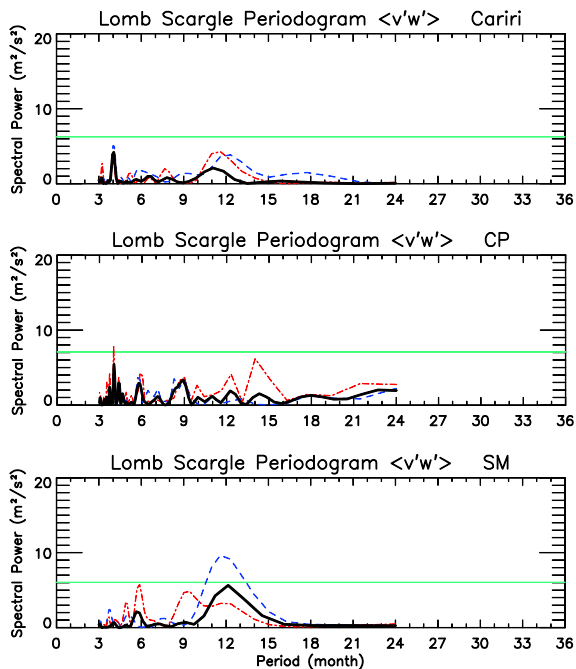
Figure 12. The same as Fig. 11 but for the meridional momentum flux component.

been suggested. Nevertheless, Yuan et al. (2010) reported a 4-month oscillation in their seasonal analysis of NmF2 ionosonde data from 33 stations at three different longitudes from 1969 to 1986. They also found a good phase match between annual and semiannual oscillations as well as for the terannual oscillation; on this basis they concluded that the terannual oscillation could be the response to a nonlinear interaction between annual and semiannual oscillations. Nevertheless, this is not applicable to our analysis since there are no occurrences of both semiannual and annual oscillations simultaneously for momentum fluxes, neither for CP nor for SM.

5 Summary

In this work we present a seasonal analysis of GW momentum fluxes and variances at different latitudes in the MLT region obtained by meteor radar observations at 7, 23 and 30° S. Analysis of variability in the $<u'w'>$ component showed a 12-month oscillation with maximum positive flux in June over the three latitudes analyzed, and a 4-month oscillation at 92.5 km over SM. On the other hand, the $<v'w'>$ component showed a 4-month oscillation at 92.5 km over CP with maximum positive fluxes in February, June and October, and an annual oscillation at 89 km over SM with maximum positive fluxes around winter. Seasonal analyses of the GW variances have also revealed an annual oscillation present at CP and SM for almost all altitudes in both components and a semiannual oscillation, mainly in the meridional component

at CP and SM, and of the zonal component at the three sites at certain altitudes. These annual and semiannual oscillations in the GW activity have been reported by several other authors at different latitudes and different altitudes. However, more studies are necessary to explain the 4-month oscillations observed over these sites.

Experimental results on the latitudinal dependence of GW momentum fluxes at low latitudes with ground-based instruments in the MLT region have not been reported up to now. Worldwide measurements of these parameters are important for the improvement of our understanding of the atmosphere and will help in the testing of future general circulation models.

References

Andrioli, V. F., Fritts, D. C., Batista, P. P., and Clemesha, B. R.: Improved analysis of all-sky meteor radar measurements of gravity wave variances and momentum fluxes, Ann. Geophys., 31, 889–908, doi:10.5194/angeo-31-889-2013, 2013a.

Andrioli, V. F., Fritts, D. C., Batista, P. P., Clemesha, B. R., and Janches, D.: Diurnal variation in gravity wave activity at low and middle latitudes, Ann. Geophys., 31, 2123–2135, doi:10.5194/angeo-31-2123-2013, 2013b.

Antonita, T. M., Ramkumar, G., Kumar, K. K., and Deepa, V.: Meteor wind radar observations of gravity wave momentum fluxes and their forcing toward the Mesospheric Semiannual Oscillation, J. Geophs. Res., 113, D10115, doi:10.1029/2007JD009089, 2008.

Beldon, C. L. and Mitchell, N. J.: Gravity waves in the mesopause region observed by meteor radar, 2: Climatologies of gravity waves in the Antarctic and Arctic, J. Atmos. Sol.-Terr. Phy., 71, 875–884, doi:10.1016/j.jastp.2009.03.009, 2009.

Clemesha, B. R., Batista, P. P., Buriti da Costa, R. A., and Schuch, N.: Seasonal variations in gravity wave activity at three locations in Brazil, Ann. Geophys., 27, 1059–1065, doi:10.5194/angeo-27-1059-2009, 2009.

de Wit, R. J., Hibbins, R. E., Espy, P. J., Orsolini, Y. J., Limpasuvan, V., and Kinnison, D. E.: Observations of gravity wave forcing of the mesopause region during the January 2013 major Sudden Stratospheric Warming, Geophys. Res. Lett., 41, 4745–4752, doi:10.1002/2014GL060501, 2014a.

de Wit, R. J., Hibbins, R. E., and Espy, P. J.: The seasonal cycle of gravity wave momentum flux and forcing in the high latitude northern hemisphere mesopause region, J. Atmos. Sol.-Terr. Phy., 127, 21–29, doi:10.1016/j.jastp.2014.10.002, 2014b.

Fritts, D. and Alexander, M. J.: Gravity wave dynamics and effects in the middle atmosphere, Rev. Geophys., 41, 1003, doi:10.1029/2001RG000106, 2003.

Fritts, D. C., Janches, D., and Hocking, W. K.: Southern Argentina Agile Meteor Radar: Initial assessment of gravity wave momentum fluxes, J. Geophys. Res., 115, D19123, doi:10.1029/2010JD013891, 2010.

Fritts, D. C., Janches, D., Hocking, W. K., Bageston, J. V., and Leme, N. M. P.: Drake Antarctic Agile Meteor Radar (DrAAMER) First Results: Configuration and Comparison of Mean and Tidal Wind and Gravity Wave Momentum Flux Measurements with SAAMER, J. Geophs. Res., 117, D02105, doi:10.1029/2011JD016651, 2012a.

Fritts, D. C., Janches, D., Hocking, W. K., Mitchell, N. J., and Taylor, M. J.: Assessment of gravity wave momentum flux measurement capabilities by meteor radars having different transmitter power and antenna configurations. J. Geophys. Res., 117, D10108, doi:10.1029/2011JD017174, 2012b.

Fukuyama, K.: Airglow variations and dynamics in the lower thermosphere and upper mesosphere – II. Seasonal and long-term variations, J. Atmos. Sol.-Terr. Phy., 39, 1–14, 1977.

Hall, C. M., Nozawa, S., Meek, C. E., Manson, A. H., and Luo, Y.: Periodicities in energy dissipation rates in the auroral mesosphere/lower thermosphere, Ann. Geophys., 21, 787–796, doi:10.5194/angeo-21-787-2003, 2003.

Hocking, W. K.: A new approach to momentum flux determinations using SKiYMET meteor radars, Ann. Geophys., 23, 2433–2439, doi:10.5194/angeo-23-2433-2005, 2005.

Iimura, H., Fritts, D. C., and Riggin, D. M.: Long-term oscillations of the wind field in the tropical mesosphere and lower thermosphere from Hawaii MF radar measurements, J. Geophys. Res.-Atmos., 115, D09112, doi:10.1029/2009JD012509, 2010.

Lindzen, R. S.: Turbulence and stress owing to gravity wave and tidal breakdown, J. Geophs. Res., 86, 9707–9714, 1981.

Mitchell, N. J. and Beldon, C. L.: Gravity waves in the mesopause region observed by meteor radar: 1. A simple measurement technique, J. Atmos. Sol.-Terr. Phy., 71, 866–874, doi:10.1016/j.jastp.2009.03.011, 2009.

Placke, M., Stober, G., and Jacobi, C.: Gravity wave momentum fluxes in the MLT – Part I: Seasonal variation at Collm (51.31° N, 13.01° E), J. Atmos. Sol.-Terr. Phy., 73, 904–910, doi:10.1016/j.jastp.2010.07.012, 2011a.

Placke, M., Hoffmann, P., Becker, E., Jacobi, C., Singer, W., and Rapp, M.: Gravity wave momentum fluxes in the MLT – Part II: Meteor radar investigations at high and midlatitudes in comparison with modeling studies, J. Atmos. Sol.-Terr. Phy., 73, 911–920, doi:10.1016/j.jastp.2010.05.007, 2011b.

Sato, K., Watanabe, S., Kawatani, Y., Tomikawa, Y., Miyazaki, K., and Takahashi, M.: On the origins of mesospheric gravity waves, Geophs. Res. Lett., 36, L19801, doi:10.1029/2009GL039908, 2009.

Sato, K., Tateno, S., Watanabe, S., and Kawatani, Y.: Gravity Wave Characteristics in the Southern Hemisphere Revealed by a High-Resolution Middle-Atmosphere General Circulation Model, J. Atmos. Sci., 69, 1378–1396,. 2011.

Scargle, J. D.: Studies in astronomical time series analysis. II – Statistical aspects of spectral analysis of unevenly spaced data, Astrophys. J., Part 1, 263, 835–853, 1982.

Senft, D. C. and Gardner, C. S.: Seasonal variability of gravity wave activity and spectra in the mesopause region at Urbana, J. Geophys. Res., 96, 17229–17264, 1991.

Yuan, W., Xu, J., Ma, R., Wu, Q., Jiang, G., Gao, H., Liu, X., and Chen, S.: First observation of mesospheric and thermospheric winds by a Fabry-Perot interferometer in China, Chinese Sci. Bull., 55, 4046-4051, 2010.